Activation of AMP-Activated Protein Kinase Inhibits Oxidized LDL-Triggered Endoplasmic Reticulum Stress In Vivo

Yunzhou Dong,[1] Miao Zhang,[1] Shuangxi Wang,[1] Bin Liang,[1] Zhengxing Zhao,[1] Chao Liu,[1] Mingyuan Wu,[1] Hyoung Chul Choi,[2] Timothy J. Lyons,[1] and Ming-Hui Zou[1]

OBJECTIVE—The oxidation of LDLs is considered a key step in the development of atherosclerosis. How LDL oxidation contributes to atherosclerosis remains poorly defined. Here we report that oxidized and glycated LDL (HOG-LDL) causes aberrant endoplasmic reticulum (ER) stress and that the AMP-activated protein kinase (AMPK) suppressed HOG-LDL–triggered ER stress in vivo.

RESEARCH DESIGN AND METHODS—ER stress markers, sarcoplasmic/endoplasmic reticulum Ca^{2+} ATPase (SERCA) activity and oxidation, and AMPK activity were monitored in cultured bovine aortic endothelial cells (BAECs) exposed to HOG-LDL or in isolated aortae from mice fed an atherogenic diet.

RESULTS—Exposure of BAECs to clinically relevant concentrations of HOG-LDL induced prolonged ER stress and reduced SERCA activity but increased SERCA oxidation. Chronic administration of Tempol (a potent antioxidant) attenuated both SERCA oxidation and aberrant ER stress in mice fed a high-fat diet in vivo. Likewise, AMPK activation by pharmacological (5′-aminoimidazole-4-carboxymide-1-β-D-ribofuranoside, metformin, and statin) or genetic means (adenoviral overexpression of constitutively active AMPK mutants) significantly mitigated ER stress and SERCA oxidation and improved the endothelium-dependent relaxation in isolated mouse aortae. Finally, Tempol administration markedly attenuated impaired endothelium-dependent vasorelaxation, SERCA oxidation, ER stress, and atherosclerosis in $ApoE^{-/-}$ and $ApoE^{-/-}$/AMPKα$2^{-/-}$ fed a high-fat diet.

CONCLUSION—We conclude that HOG-LDL, via enhanced SERCA oxidation, causes aberrant ER stress, endothelial dysfunction, and atherosclerosis in vivo, all of which are inhibited by AMPK activation. ***Diabetes*** **59:1386–1396, 2010**

LDL oxidation and glycation are known to promote atherosclerosis through several mechanisms that include promoting vascular proinflammatory responses, intracellular oxidative stress, and apoptosis associated with endothelial dysfunction (1,2). In addition, LDL oxidation is greatly enhanced by LDL glycation (3,4). For example, glycation of LDL slows the clearance of these particles from the circulation (5), increases their susceptibility to oxidative damage (6), enhances entrapment of extravasated particles in the vascular subintimal space, and increases chemotactic activity of monocytes (7). The presence of both glycated LDL and glycoxidized LDL in human atherosclerotic plaques has been confirmed by immunochemical methods both in vivo and in vitro (8–10). Increasing evidence suggests that glycation and oxidation of LDL induces apoptosis in arterial wall cells (11,12), and glycoxidized LDL triggers apoptosis in vascular smooth muscle cells (13,14). Overall, glycation of LDL promotes the formation of oxidized LDL, and this phenomenon contributes to accelerated atherosclerosis, an important pathologic corollary of diabetes.

Endoplasmic reticulum (ER) stress has been linked to a wide range of human pathologies including diabetes (15–17), obesity (16,17), atherosclerosis (18), cancer, neurodegenerative disorders, and inflammatory conditions. ER stress may be triggered by high glucose, oxidative stress, Ca^{2+} overload, ischemia, and hypoxia. In addition, it causes the accumulation of unfolded and misfolded proteins, leading to an "unfolded protein response" (19). The normal ER is the principal site of protein synthesis, folding, and maturation. In unfolded protein response, unfolded or misfolded proteins are sent to the cytoplasm by a "retro-translocation mechanism" to be degraded by the ubiquitin proteasome system (20).

AMP-activated protein kinase (AMPK), a sensor of cellular energy status, plays a critical role in controlling the cell's energy balance and metabolism (21), and activation of AMPK is an important defensive response to stress (22). AMPK activation is neuroprotective (23), and also mediates at least some cardiovascular protective effects of drugs such as hydroxymethylglutaryl-CoA reductase inhibitors (e.g., the statins such as pravastatin and atorvastatin) and metformin (a biguanide that activates AMPK) (24,25). Activation of AMPK protects cardiomyocytes against hypoxic injury through attenuation of ER stress (26). However, whether AMPK alters oxidized LDL-induced ER stress in endothelial cells has not been investigated to date. In this study, we report that oxidized, glycated-LDL (HOG-LDL) via the oxidation and inhibition of sarcoplasmic/endoplasmic reticulum Ca^{2+} ATPase (SERCA), triggers ER stress in endothelial cells in vivo. In addition, we have uncovered evidence suggesting that AMPK activation attenuates ER stress by inhibiting SERCA oxidation caused by HOG-LDL.

From the [1]Section of Endocrinology and Diabetes, University of Oklahoma Health Sciences Center, Oklahoma City, Oklahoma; and the [2]Department of Pharmacology, College of Medicine, Yeungnam University, Daegu, Korea.
Corresponding author: Ming-Hui Zou, ming-hui-zou@ouhsc.edu.
Received 7 November 2009 and accepted 24 February 2010. Published ahead of print at http://diabetes.diabetesjournals.org on 18 March 2010. DOI: 10.2337/db09-1637.
Y.D. and M.Z. contributed equally to this study.

RESEARCH DESIGN AND METHODS

Materials. Antibodies against phospho-AMPK, phospho-acetyl-CoA carboxylase (ACC), phospho-eukaryotic translation initiation factor 2α (eIF2α), anti-endothelial nitric oxide synthase, phospho–Jun NH_2-terminal kinase (JNK), and 3-nitrotryosine were obtained from Cell Signaling Biotechnology (Danvers, MA). The antibodies against phospho-PKR (protein kinase R)-like ER kinase (PERK), X-box binding protein 1 (XBP-1), and SERCA, scrambled small interfering RNA (siRNA), and the specific siRNA for calcium/calmodulin-dependent protein kinase kinase 2 (CaMKK2), SERCA2, and $p67^{phox}$ were obtained from Santa Cruz Biotechnology Inc. (Santa Cruz, CA). Antibodies against glucose-regulated protein 78 (GRP78) and oxidized LDL (ox-LDL) were from Abcam (Cambridge, MA). Antibody against activating transcription factor 6 (ATF6) was obtained from Imgenex (San Diego, CA). 3-(4-morpholinyl)sydnone imine hydrochloride (SIN-1) was from Dojindo Laboratories USA (Rockville, MD). 5′-aminoimidazole-4-carboxymide-1-β-D-ribofuranoside (AICAR) was from Toronto Research Chemicals Inc. (North York, ON, Canada). Fluo-4 NW kits were obtained from Invitrogen Inc. (Carlsbad, CA). All other chemicals, if not indicated, were purchased from Sigma-Aldrich (St. Louis, MO).

Animals. All mice were housed in temperature-controlled cages under a 12-h light-dark cycle and given free access to water and normal chow. $AMPK\alpha2^{-/-}$ mice that had been backcrossed onto a C57BL/6 background were crossed with $ApoE^{-/-}$ mice (The Jackson Laboratory), also on the C57BL/6 background, to generate $ApoE^{-/-}/AMPK\alpha2^{-/-}$ mice. Accelerated atherosclerosis was induced by feeding the mice a Western diet containing 0.21% cholesterol and 21% fat (D12079B; Research Diets Inc.). This diet was administered beginning at 5 weeks of age and continued for 8 consecutive weeks. At 5 weeks of age, Tempol (Sigma-Aldrich) was also added to the drinking water (1 mmol/l) for 8 weeks. $ApoE^{-/-}$ mice fed with normal chow were used as controls. The animal protocol was reviewed and approved by the University of Oklahoma Institutional Animal Care and Use Committee.

Preparation of N-LDL and oxidized and glycated LDL. Native LDL (N-LDL) and HOG-LDL were prepared as described previously (27). Final preparations were dialyzed extensively against PBS buffer. Characterization of native and HOG-LDL was done by gel electrophoresis (fluorescence at 360 nm excitation/430 nm emission, and absorbance at 234 nm, as described previously [27,28]). The study protocol was approved by the Institutional Review Board at the University of Oklahoma Health Sciences Center.

Cell culture and treatment. Both bovine aortic endothelial cells (BAECs) and human umbilical vein endothelial cells (HUVECs) were cultured in endothelial basal medium with 2% FBS. After confluence, cells were incubated with HOG-LDL at the concentrations and times indicated. Cells exposed to the same concentrations of N-LDL were used as controls. If needed, pharmacological reagents, including 1,2-B is BAPTA-AM (10 μmol/l), AICAR (1 mmol/l), or Tempol (10 μmol/l), were added 30 min prior to the addition of N-LDL or HOG-LDL.

Downregulation of gene expression by siRNA. Confluent HUVECs were transfected with control or gene-specific siRNA according to manufacturer's recommendations. To improve suppression of the target gene, two rounds of consecutive siRNA gene silencing were performed. The efficiency of siRNA-silenced genes was evaluated by Western blotting of the targeted protein with specific antibodies.

Adenoviral preparation and infection. Adenoviral vector AMPK-CA (a constitutively active AMPK mutant) was generated as previously reported (25). Adenoviral vector AMPK-DN (a dominant-negative mutant of AMPK) was generated by subcloning the cDNA encoding AMPKα1-DN-(D159A) into adenoviral vector pAdEasy-1.

Confluent cells were infected with adenoviruses at multiplicity of infection of 50 for 36 h, as described previously (25). Adenovirus encoding green fluorescent protein (GFP) was used as control. Under this condition, the expression efficiency was >80% as seen by GFP expression.

Preparation of cytosolic and membrane fractions. Cellular cytosolic and membrane fractions were prepared as described previously (25). Translocation of $p47^{phox}$ subunit of NAD(P)H oxidase was determined in Western blot.

Assays of the endothelium-dependent and –independent vasorelaxation. The endothelium-dependent (assays of bioactive nitric oxide [NO]) and -independent (assays of vascular smooth muscle responsiveness to nitric oxide donor sodium nitroprusside) vasorelaxation was measured as described previously (27).

Measurement of intracellular $[Ca^{2+}]_i$, SERCA activity, cysteine 674 labeling, and ratiometric analysis of SERCA function. Intracellular calcium concentration ($[Ca^{2+}]_i$) was measured using a Fluo-4 NW kits in accordance with manufacturer's recommendations with the fluorophore excited at 485 nm and detection at 520 nm (27). $[Ca^{2+}]_i$ was expressed as a percentage of control. SERCA activity was measured as described previously (29). Biotinylated-iodoacetamide (b-IAM) labeling of SERCA cysteine 674 was performed according to the methods described by Tong et al. (30). Proteins were separated by SDS-PAGE, and b-IAM labeled Cys674-SERCA was detected using SERCA-specific antibody. Ratiometric Ca^{2+} measurement, which can assay SERCA function dynamically, was conducted as described previously (31).

Determination of serum cholesterol, triglyceride, and blood glucose levels. Mice underwent a 14- to 15-h fast before blood samples were collected. Blood glucose levels were determined by applying tail blood to an OneTouch Ultra Blood Glucose Monitoring System (LifeScan). Serum cholesterol and triglyceride levels were measured enzymatically, using Infinity reagents from Thermo DMA according to the manufacturer's instructions.

Atherosclerotic lesion analysis. After being fed the Western diet for 8 weeks, mice were fasted for 14 h and then were anesthetized and killed. The heart and aortic tissue were removed from the ascending aorta to the ileal bifurcation and placed in 4% paraformaldehyde for 16 h. For analyzing the lesion area in the aortic root, the heart was dissected from the aorta, embedded in Polyfreeze tissue freezing medium (Polysciences, Inc.), and sectioned (5-μm thickness). Four sections representing every tenth serial section over a distance of 200 μm were collected from each mouse and stained with Oil Red O for neutral lipids, and counterstained with hematoxylin to visualize the nuclei. Plaques were imaged with an Olympus microscope connected to a QImaging Retiga CCD camera. The aortic lesion size of each animal was obtained by the averaging of lesion areas in four sections from the same mouse. For analyzing the lesion area in the aortic arch, the intimal surface was exposed by a longitudinal cut from the ascending arch to 5 mm distal of the left subclavian artery to allow the lumen of the aortic arch to be laid flat. The aorta was rinsed for 5 min in 75% ethanol, stained with 0.5% Sudan IV in 35% ethanol and 50% acetone for 15 min, destained in 75% ethanol for 5 min, and then rinsed with distilled water. Digital images of the aorta were captured under a stereomicroscope, and the lesion area was quantified from the aortic arch to 5 mm distal of the left subclavian artery using Alpha Ease FC software (Version 4.0; Alpha Innotech).

Immunocytochemistry staining. Immunocytochemistry stainings for oxidized LDL and ER stress markers were performed as described previously (32).

Statistics. Results were analyzed with a one-way ANOVA with appropriate post hoc analysis of results as well as Student *t* test. Values were expressed as mean ± SD. $P < 0.05$ was considered statistically significant.

RESULTS

HOG-LDL increases ER stress in endothelial cells. We had previously reported (27) that exposure of BAECs to HOG-LDL impairs endothelial function by inducing calpain-mediated endothelial NO synthase degradation in a reactive oxygen species (ROS)– and Ca^{2+}-dependent manner. Whether HOG-LDL alters ER stress was not known. To determine the effect of HOG-LDL on ER stress, confluent BAECs were exposed to HOG-LDL at a concentration of 100 μg/ml, which is considered to be pathologically relevant to type 2 diabetes (28), for 30 min to 6 h. BAECs exposed to N-LDL (100 μg/ml) were used as controls. As depicted in Fig. 1*A*, HOG-LDL but not N-LDL, markedly increased the detection of p-PERK and p-eIF2α, two established ER stress markers, as early as 30 min after HOG-LDL exposure. Concomitantly, HOG-LDL also increased the expression of GRP78 and the cleavage of ATF6 (Fig. 1*A*).

The effects of HOG-LDL appeared to be dose dependent. Low concentration of HOG-LDL (50 μg/ml) markedly increased the detection of p-PERK, p-eIF2α, and p-JNK in BAECs at 6 h (Fig. 1*B* and *C*). ER stress markers (p-PERK, p-eIF2α, and p-JNK) increased as the doses of LDL increased (25–200 μg/ml) within 6-h exposure.

Ca^{2+}chelation abolishes HOG-LDL–induced ER stress. Because exposure of BAECs to HOG-LDL elevates intracellular calcium $[Ca^{2+}]_i$ in BAECs (27), we next determined whether the rise of $[Ca^{2+}]_i$ contributed to increased detection of ER stress. We first determined whether calcium mobilizing reagents triggered ER stress in BAECs. As expected, exposure of BAECs to calcimycin, a well-known Ca^{2+} mobilizer, markedly increased the detection of ER

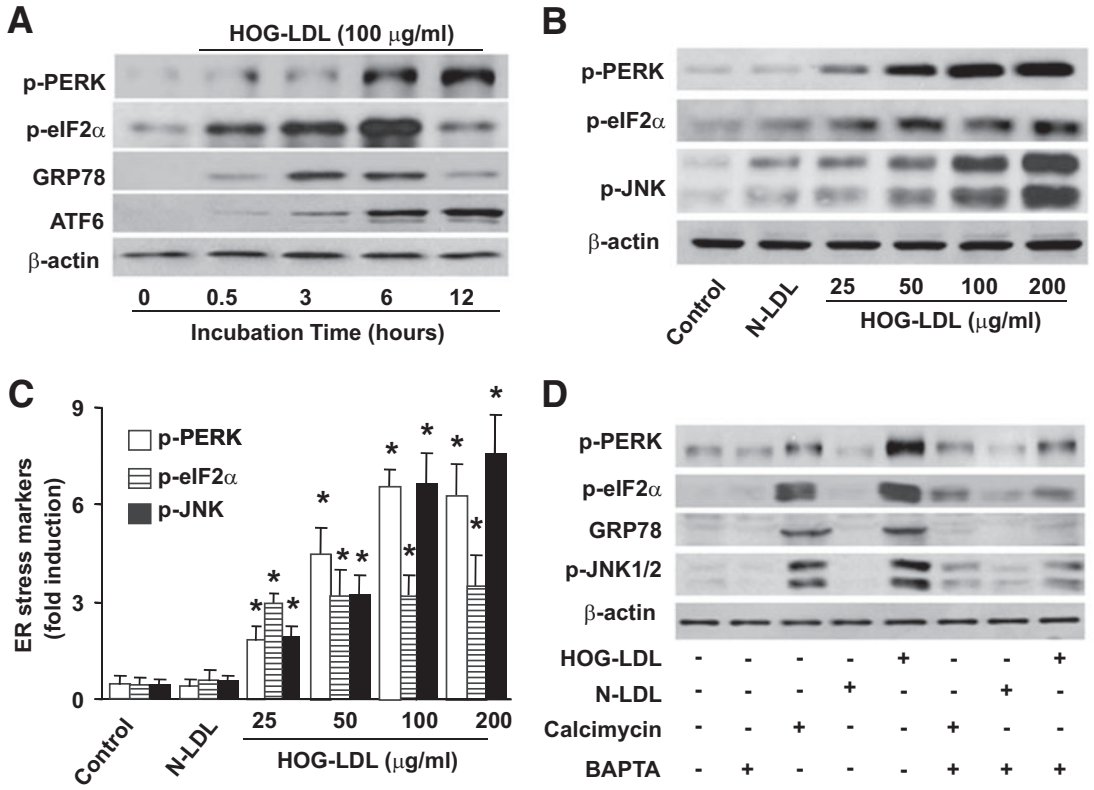

FIG. 1. HOG-LDL induces prolonged ER stress in a Ca^{2+}-dependent manner. *A*: Time-dependent ER stress by HOG-LDL in BAECs. $n = 3$. *B* and *C*: HOG-LDL induced ER stress in a dose-dependent manner within 6 h of treatment. $n = 3$. *$P < 0.05$ vs. controls in each group. *D*: HOG-LDL–induced ER is dependent on elevation of intracellular Ca^{2+}. $n = 3$.

stress markers (Fig. 1*D*). Consistently, tunicamycin (16), meflouquine, or SIN-1, all of which are known to increase intracellular $[Ca^{2+}]_i$, also increased ER stress in BAECs (supplementary Fig. 1, available in an online appendix at http://diabetes.diabetesjournals.org/content/early/2010/03/10/db09-1637/suppl/DC1).

It was important to determine whether chelating $[Ca^{2+}]_i$ reversed the effects of HOG-LDL on ER stress. Pretreatment of BAECs with BAPTA-AM (10 μmol/l) significantly inhibited HOG-LDL–induced ER stress (Fig. 1*D* and supplementary Fig. 1*C*), implying that a rise in $[Ca^{2+}]_i$ was critical for HOG-LDL–enhanced ER stress.

HOG-LDL–triggered ER stress is oxidative stress dependent. As peroxynitrite ($ONOO^-$) is known to increase both intracellular calcium and ER stress (33), we next determined whether $ONOO^-$ mediated the effects of HOG-LDL. 3-nitrotyrosine (3-NT)–positive proteins are considered a footprint of $ONOO^-$ in cultured cells. We first assayed whether HOG-LDL increased the levels of 3-NT. As depicted in Fig. 2*A*, exposure of BAECs to HOG-LDL, but not N-LDL, dose-dependently increased the levels of 3-NT–positive proteins, implying that HOG-LDL increased $ONOO^-$ in endothelial cells.

$ONOO^-$ is a potent oxidant formed by the combination of superoxide and NO. Our previously published data (27) demonstrate that HOG-LDL enhances both superoxide and $ONOO^-$ upon its reaction with NO by activating NAD(P)H oxidase. Therefore, it was interesting to determine whether inhibition of NAD(P)H oxidase or scavenging superoxide altered HOG-LDL–triggered ER stress. To this end, BAECs were pretreated with apocynin, a potent inhibitor for NAD(P)H oxidase, or Tempol, a superoxide scavenger, prior to the addition of HOG-LDL. As shown in Fig. 2*B*, both apocynin and Tempol significantly attenuated HOG-LDL–induced ER stress.

Next, we determined whether genetic inhibition of NAD(P)H oxidase attenuated ER stress caused by HOG-LDL. As depicted in Fig. 2*C*, transfection of $p67^{phox}$-specific siRNA significantly reduced the levels of $p67^{phox}$, an essential component of NAD(P)H oxidases. Further, transfection of $p67^{phox}$-specific siRNA, but not control siRNA, abrogated HOG-LDL–induced ER stress (Fig. 2*C* and *D*). Taken together, our results suggest that NAD(P)H oxidase–derived ROSs were required for HOG-LDL–triggered ER stress.

Inhibition of SERCA increases ER stress in endothelial cells. Because SIN-1, an $ONOO^-$ donor, increased both intracellular Ca^{2+} and ER stress (supplementary Fig. 1*B* and *C*), we next investigated how $ONOO^-$ increased intracellular Ca^{2+} in BAECs. Because SERCA is a key enzyme that controls Ca^{2+} transfer from the cytosol to the ER lumen and its inhibition is known to cause aberrant ER stress in various cell types (34), we hypothesized that $ONOO^-$ generated during HOG-LDL exposure might alter SERCA function resulting in increased levels of $[Ca^{2+}]_i$. Indeed, exposure of BAECs to thapsigargin, a specific SERCA inhibitor, triggered ER stress in both a time- and concentration-dependent manner in BAECs (supplementary Fig. 2*A* and *B*).

To avoid potential off-target effects of thapsigargin, we next determined whether genetic inhibition of SERCA2 altered ER stress in endothelial cells. Because bovine-specific SERCA siRNA is not available, we performed siRNA experiments in HUVECs, in which HOG-LDL caused a Tempol-sensitive aberrant ER stress and SERCA inhibition (supplementary Fig. 3). As expected, gene si-

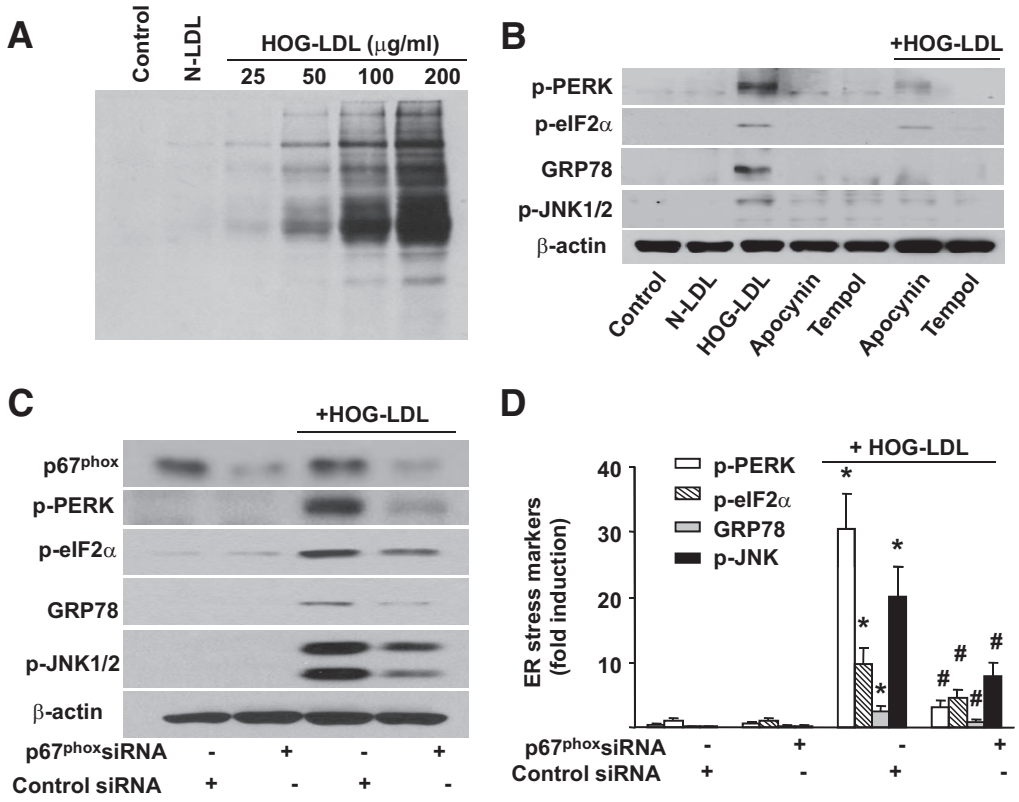

FIG. 2. HOG-LDL–triggered ER stress is oxidative stress dependent. BAECs were treated with different concentration of HOG-LDL (0–100 μg/ml) for 6 h, as described in the "Research Design and Methods" section. *A*: HOG-LDL increases the detection of 3-NT–positive proteins. 3-NT–positive protein was detected in Western blot using 3-NT–specific antibody; $n = 3$. *B*: Effect of inhibition of NAD(P)H oxidase and ROS scavengers on HOG-LDL–induced ER stress. BAECs were pretreated with apocynin (100 μmol/l) or Tempol (10 μmol/l), followed by HOG-LDL treatment as indicated. $n = 4$. *C* and *D*: Gene silencing of $p67^{phox}$ of NAD(P)H oxidase attenuates ER stress induced by HOG-LDL in HUVECs; $n = 6$. *$P < 0.05$ control siRNA cells vs. control siRNA plus HOG-LDL; #$P < 0.05$ control siRNA plus HOG-LDL vs. $p67^{phox}$ siRNA plus HOG-LDL.

lencing of SERCA2 markedly increased HOG-LDL–induced ER stress in endothelial cells (supplementary Fig. 2*C* and *D*), suggesting SERCA inhibition triggered ER stress in endothelial cells.

HOG-LDL reduces SERCA activity along with increased detection of SERCA oxidation. To explore how HOG-LDL exposure could trigger ER stress in endothelial cells, we first determined whether HOG-LDL suppressed SERCA activity. As depicted in Fig. 3*A*, HOG-LDL significantly inhibited SERCA activity in BAECs. However, HOG-LDL had no effect on the expression of SERCA(s) in endothelial cells (Fig. 3*B*), suggesting that HOG-LDL–induced suppression of SERCA activity was independent of transcriptional and translational regulation of SERCA.

Because Cys674 of SERCA is reported to be oxidized and suppressed by ROSs (30), we next determined whether HOG-LDL increased the SERCA oxidation at Cys674. We first determined whether inhibition of NAD(P)H oxidase with apocynin or scavenging superoxide with Tempol, both of which suppressed HOG-LDL–induced ER stress (Fig. 2*B*), also alleviated the effects of HOG-LDL on SERCA activity and SERCA oxidation on Cys674. As depicted in Fig. 3*A*, Tempol restored SERCA activity in HOG-LDL–treated cells. Similarly, apocynin ablated the reduction in SERCA activity induced by HOG-LDL (Fig. 3*C*). Consistently, HOG-LDL significantly increased oxidation of Cys674 (Fig. 3*D*). Furthermore, Tempol prevented HOG-LDL–enhanced SERCA oxidation (Fig. 3*D*). Cumulatively, these findings suggest that HOG-LDL attenuates SERCA activity via ROS-mediated oxidation of the Cys674 residue of these ATPases.

AICAR restores intracellular calcium and SERCA activity but suppresses ER stress. We had reported that AMPK activation by AICAR reduces oxidative stress in diabetes (35). It was therefore interesting to investigate whether AMPK activation alleviated SERCA oxidation and consequent ER stress caused by HOG-LDL. Short exposure (<3 h) of BAECs to HOG-LDL (100 μg/ml) markedly increased the detection of AMPK phosphorylation at Thr172 (Fig. 4*A*), an index for AMPK activation. AICAR significantly enhanced AMPK Thr172 phosphorylation caused by HOG-LDL alone (Fig. 4*A*).

We next determined whether the reduction of ER stress was via a reduction of $[Ca^{2+}]_i$. As depicted in Fig. 4*B*, AICAR blocked HOG-LDL–induced $[Ca^{2+}]_i$ rise and reduced the markers of ER stress (Fig. 4*C*).

As apocynin ablated HOG-LDL–induced ER stress and SERCA oxidation, it was logical to determine whether AMPK activation by AICAR lowered HOG-LDL–induced ER stress by suppressing the activation of NAD(P)H oxidase. As depicted in Fig. 4*D*, HOG-LDL exposure increased the membrane translocation of $p47^{phox}$, a key step for NAD(P)H oxidase assembly and activation. Importantly, AICAR suppressed the effects of HOG-LDL on $p47^{phox}$ translocation (Fig. 4*D*).

We next assayed whether AICAR attenuated SERCA inhibition caused by HOG-LDL. AMPK activation by AICAR inhibited HOG-LDL–induced reduction in SERCA activity in BAECs (Fig. 4*E*). To further confirm the effect of AICAR on SERCA function, $[Ca^{2+}]_i$ was monitored using ratiometric measurements dynamically (31). As shown in Fig. 4*F*, compared with N-LDL–treated cells, HOG-LDL–

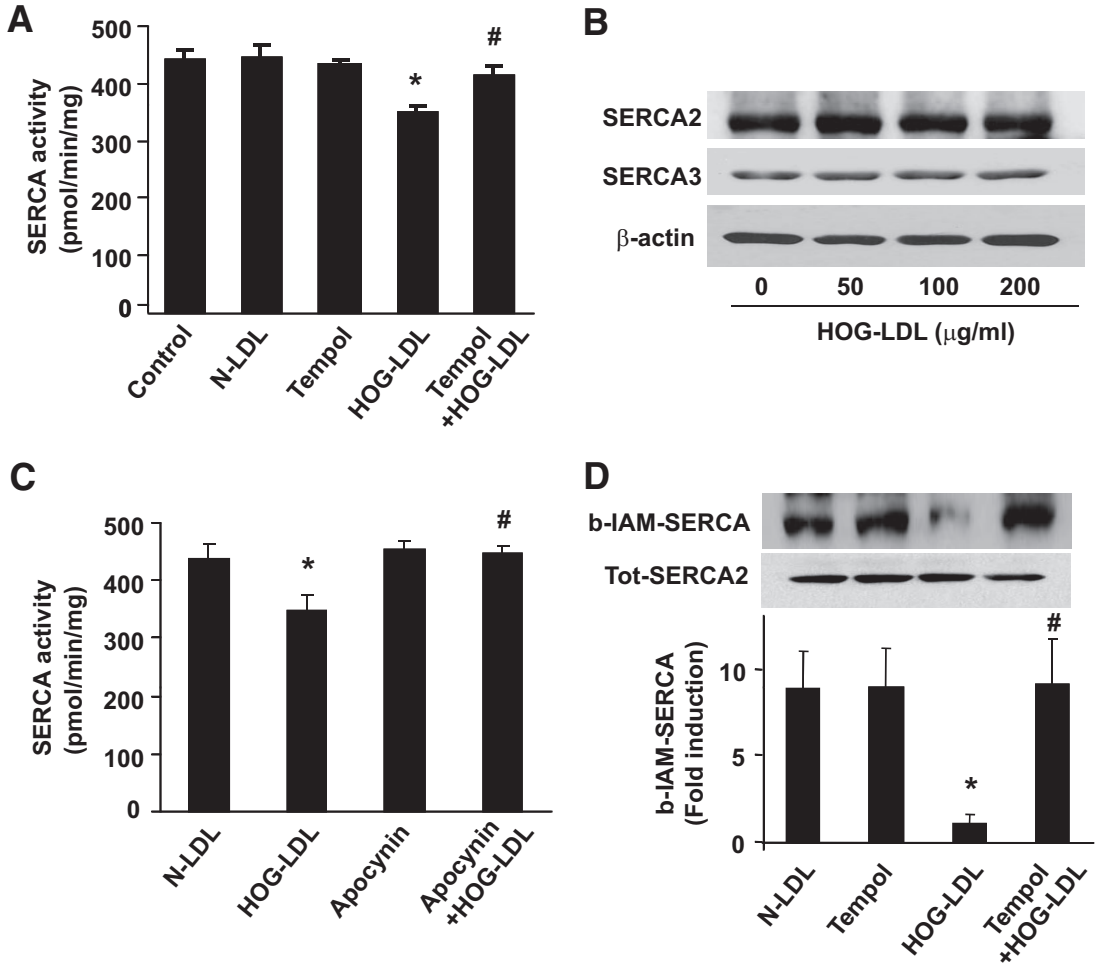

FIG. 3. HOG-LDL decreased SERCA activity by oxidation. *A*: Antioxidant Tempol attenuates the reduction of SERCA activity caused by HOG-LDL in BAECs. $n = 4$. *$P < 0.05$ HOG-LDL vs. n-LDL; #$P < 0.05$ Tempol plus HOG-LDL vs. HOG-LDL. *B*: HOG-LDL does not change SERCA(s) expression. $n = 3$. *C*: Apocynin mitigates the reduction of SERCA activity caused by HOG-LDL. $n = 4$. *$P < 0.05$ HOG-LDL vs. n-LDL; #$P < 0.05$ apocynin plus HOG-LDL vs. HOG-LDL. *D*: Antioxidant Tempol attenuates SERCA oxidation triggered by HOG-LDL in BAECs. SERCA oxidation was detected using b-IAM labeling. $n = 4$. *$P < 0.05$ HOG-LDL vs. N-LDL; #$P < 0.05$ Tempol plus HOG-LDL vs. HOG-LDL.

treated BAECs exhibited impaired ability to transfer $[Ca^{2+}]_i$ to the ER lumen, which is in line with an earlier report (28). Importantly, AICAR pretreatment abolished the effects of HOG-LDL (Fig. 4*F*). These data further support that AICAR alleviates the reduction of SERCA function caused by HOG-LDL.

AMPK protects SERCA activity and consequent ER stress caused by HOG-LDL. To exclude potential off-target effects of AICAR, we tested whether genetic activation or inhibition of AMPK modulates HOG-LDL–induced ER stress. Overexpression of AMPK-CA, a constitutively active AMPK mutant, suppressed HOG-LDL– and calcimycin-induced ER stress (Fig. 5*A* and *B*). Conversely, AMPK inhibition by overexpression of AMPK-DN, an AMPK dominant negative mutant, significantly accentuated ER stress induced by either HOG-LDL or calcimycin (Fig. 5*C* and *D*). Concomitantly, overexpression of AMPK-CA maintained SERCA activity when challenged with HOG-LDL, whereas AMPK-DN failed to maintain SERCA activity (Fig. 5*E*). Taken together, our results suggest that AMPK activation suppresses ER stress caused by HOG-LDL through maintaining SERCA activity.

AMPK activation abolishes HOG-LDL–induced ER stress in isolated mouse aorta ex vivo. To further test the role of AMPK in response to HOG-LDL–induced ER stress and consequent vascular dysfunction, we assayed the effects of metformin and statins, two clinically used AMPK activators, in isolated aortas ex vivo. Metformin or simvastatin was added 30 min prior to HOG-LDL exposure. As shown in Fig. 6*A*, both metformin and statin treatment activated AMPK when aortic rings were incubated with or without HOG-LDL. HOG-LDL induced ER stress, as indicated by stress markers p-PERK and p-eIF2α (Fig. 6*B*). Pretreatment of isolated aortae with metformin or statins ablated the effects of HOG-LDL on ER stress (Fig. 6*B* and *C*).

Next, we assessed the effects of AMPK activation on acetylcholine (ACh)–induced endothelium-dependent relaxation under ex vivo conditions. As indicated in Fig. 6*D*, HOG-LDL impaired ACh-induced relaxation. Pretreatment with metformin or simvastatin, which did not alter basal ACh-induced relaxation, reversed the reduction of Ach-induced vasorelaxation caused by HOG-LDL. In addition, the endothelium-independent vasorelaxation, as assayed by monitoring vasorelaxation to sodium nitroprusside, a NO donor, was unchanged among these groups (data not shown), suggesting unchanged function of vascular smooth muscle cells in terms of NO. Overall, these results suggest that AMPK activation is sufficient to

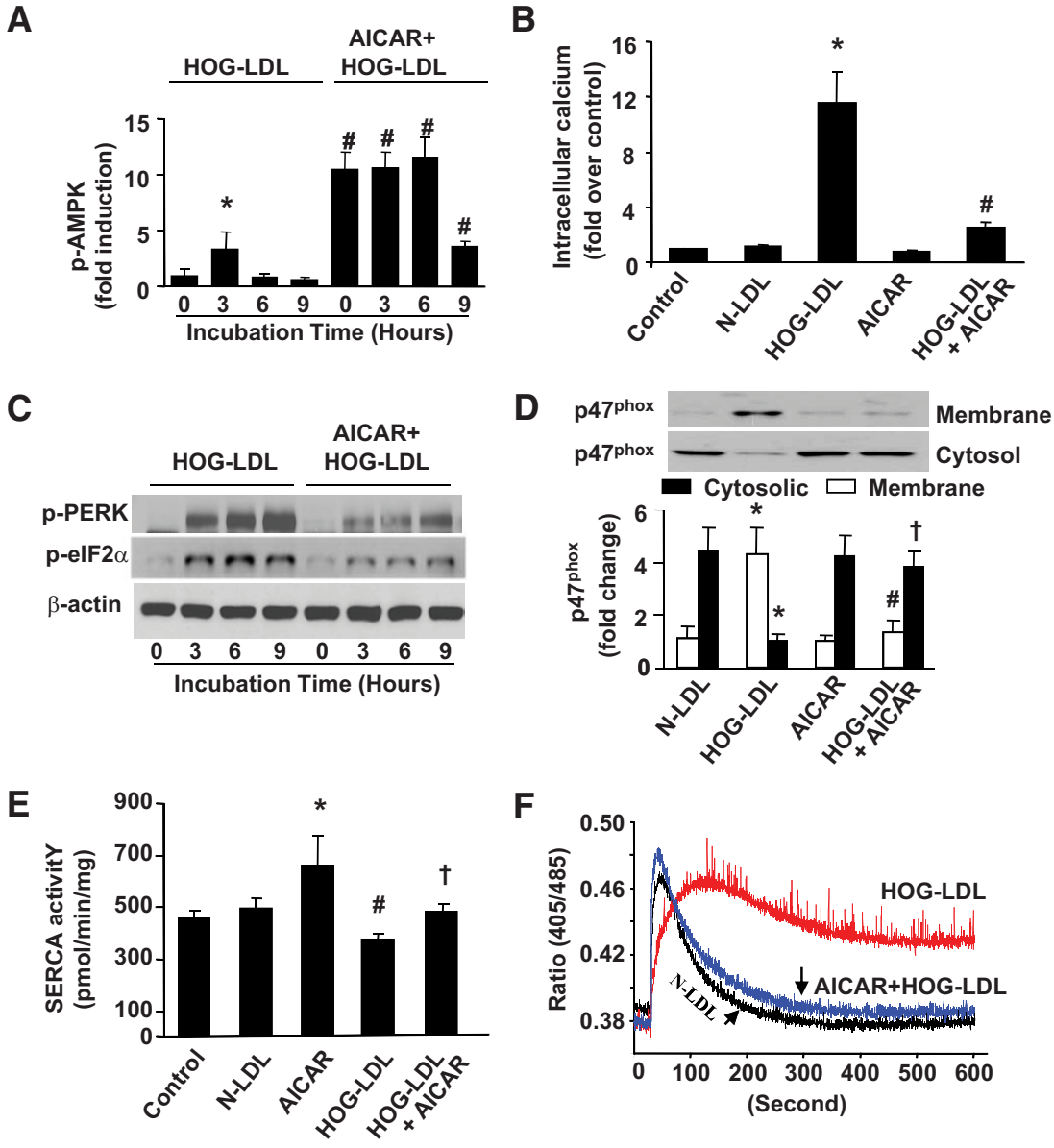

FIG. 4. AMPK activation by AICAR suppresses HOG-LDL–induced ER stress and protects SERCA activity. BAECs were treated with HOG-LDL, with or without AICAR preincubation (1 mmol/l, 30 min). *A*: AICAR increases AMPK phosphorylation at Thr172 in BAECs. $n = 3$. *$P < 0.05$ HOG-LDL-3 h vs. 0 h control; #$P < 0.01$ AICAR+HOG-LDL vs. HOG-LDL alone at times indicated. *B*: AICAR suppresses the rise of intracellular $[Ca^{2+}]_i$ in BAECs at 6 h. $n = 3$. *$P < 0.05$ HOG-LDL vs. control or N-LDL; #$P < 0.05$ HOG-LDL+AICAR vs. HOG-LDL alone. *C*: AICAR suppresses HOG-LDL–induced ER stress in BAECs. $n = 4$. *D*: AICAR pretreatment inhibited NADPH oxidase activation by blocking p47 translocation. $n = 3$. *$P < 0.05$ HOG-LDL vs. N-LDL in cytosol and membrane portion; # and † indicate $P < 0.05$ AICAR pretreatment completely blocked p47 translocation by HOG-LDL in cytosol and membrane, respectively. *E*: AICAR protects SERCA activity under HOG-LDL treatment. $n = 4$. *$P < 0.05$ AICAR treatment vs. N-LDL or control samples; #$P < 0.05$ HOG-LDL vs. N-LDL or control; †$P < 0.05$ AICAR+HOG-LDL vs. HOG-LDL alone. *F*: Ratiometric measurement of intracellular Ca^{2+}. BAECs were treated with 100 μg/ml N-LDL, 100 μg/ml HOG-LDL, and AICAR (pretreated for 30 min)+HOG-LDL for 6 h. Ratiometric measurement of intracellular Ca^{2+} was done as described in the "Research Design and Methods" section. The small arrows indicate the timing for cytosolic Ca^{2+} return to its homeostasis. $n = 6$.

preserve endothelium-dependent relaxation impaired by HOG-LDL.

AMPKα2 deletion reduces SERCA activity in parallel with ER stress in vivo. It was important to determine whether AMPK is essential in maintaining SERCA activity and inhibiting ER stress in vivo. Compared with ApoE$^{-/-}$ mice fed normal diet, ApoE$^{-/-}$ mice fed high-fat diet (HFD) had a reduced SERCA activity and exhibited greater degree of ER stress in the aorta (Fig. 7*A*–*C*). In addition, AMPKα2 depletion caused further reduction of SERCA activity with higher degree of ER stress in the aorta than ApoE counterparts (Fig. 7*A*–*C*).

Chronic administration of Tempol inhibits ER stress but protects SERCA activity. Next, we determined whether chronic administration of Tempol, a potent antioxidant, prevented SERCA oxidation and attenuated ER stress in vivo. As shown in Fig. 7*C*, Tempol treatment protected SERCA activity from reduction, suggesting that oxidation played a critical role in the reduction of SERCA activity. Importantly, Tempol markedly suppressed ER stress in both ApoE$^{-/-}$ and ApoE$^{-/-}$/AMPKα2 $^{-/-}$ mice in vivo (Fig. 7*A* and *B*). Taken together, our data imply that inhibition of SERCA oxidation is able to suppress ER stress in vivo.

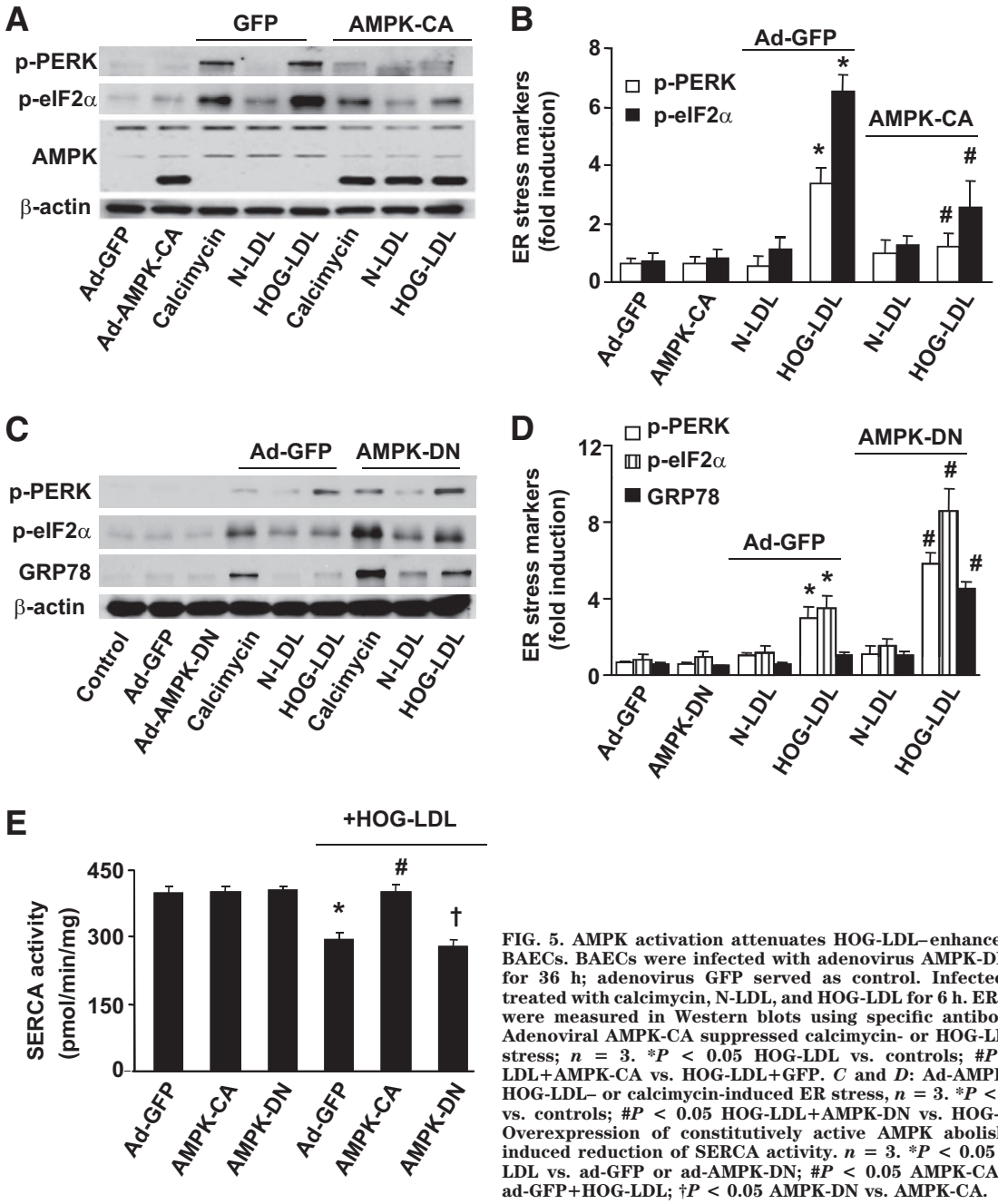

FIG. 5. AMPK activation attenuates HOG-LDL–enhanced ER stress in BAECs. BAECs were infected with adenovirus AMPK-DN or AMPK-CA for 36 h; adenovirus GFP served as control. Infected BAECs were treated with calcimycin, N-LDL, and HOG-LDL for 6 h. ER stress markers were measured in Western blots using specific antibodies. *A* and *B*: Adenoviral AMPK-CA suppressed calcimycin- or HOG-LDL–induced ER stress; $n = 3$. *$P < 0.05$ HOG-LDL vs. controls; #$P < 0.05$ HOG-LDL+AMPK-CA vs. HOG-LDL+GFP. *C* and *D*: Ad-AMPK-DN amplified HOG-LDL– or calcimycin-induced ER stress, $n = 3$. *$P < 0.05$ HOG-LDL vs. controls; #$P < 0.05$ HOG-LDL+AMPK-DN vs. HOG-LDL +GFP. *E*: Overexpression of constitutively active AMPK abolishes HOG-LDL–induced reduction of SERCA activity. $n = 3$. *$P < 0.05$ ad-GFP+HOG-LDL vs. ad-GFP or ad-AMPK-DN; #$P < 0.05$ AMPK-CA+HOG-LDL vs. ad-GFP+HOG-LDL; †$P < 0.05$ AMPK-DN vs. AMPK-CA.

Chronic administration of antioxidant Tempol improves the endothelium-dependent vasorelaxation in both ApoE$^{-/-}$ and AMPKα2$^{-/-}$/ApoE$^{-/-}$ mice. Compared with C57BL6 mice, the endothelium-dependent vasorelaxation in response to acetylcholine was normal in mice fed normal mouse chow (data not shown). The endothelium-dependent relaxation in ApoE$^{-/-}$ mice fed HFD was significantly less than those of ApoE$^{-/-}$ mice fed normal mouse chow (data not shown). In addition, the endothelium-dependent relaxation in HFD-fed ApoE$^{-/-}$/AMPKα2$^{-/-}$ mice was further reduced compared with ApoE$^{-/-}$ mice with HFD (Fig. 7*D*). Importantly, Tempol administration markedly attenuated impaired endothelium-dependent vasorelaxation in ApoE$^{-/-}$/AMPKα2$^{-/-}$ mice (Fig. 7*D*) but had no effect on the endothelium-independent vasorelaxation (data not shown).

Tempol treatment reduces ox-LDL, ER stress, and aortic lesion progression in ApoE$^{-/-}$ mice. Next, we evaluated whether Tempol altered the levels of oxidized LDL, ER stress, and aortic lesions in ApoE$^{-/-}$ mice. Compared with normal diet, HFD significantly increased ox-LDL, ER stress, and aortic lesion in ApoE$^{-/-}$ mice (Fig. 7*E* and *F*). Further, Tempol reduced the levels of oxidized LDL, ER stress markers, and aortic lesion areas (Fig. 7*E* and *F*).

Tempol does not affect serum lipid or blood glucose levels. Next, we compared metabolic parameters among ApoE$^{-/-}$ and ApoE$^{-/-}$/AMPKα2$^{-/-}$ mice. No differences in blood glucose, serum cholesterol, and triglyceride were observed between ApoE$^{-/-}$/AMPKα2$^{-/-}$ and ApoE$^{-/-}$ mice (Table 1). Tempol treatment did not affect blood glucose and triglyceride levels in both groups but in-

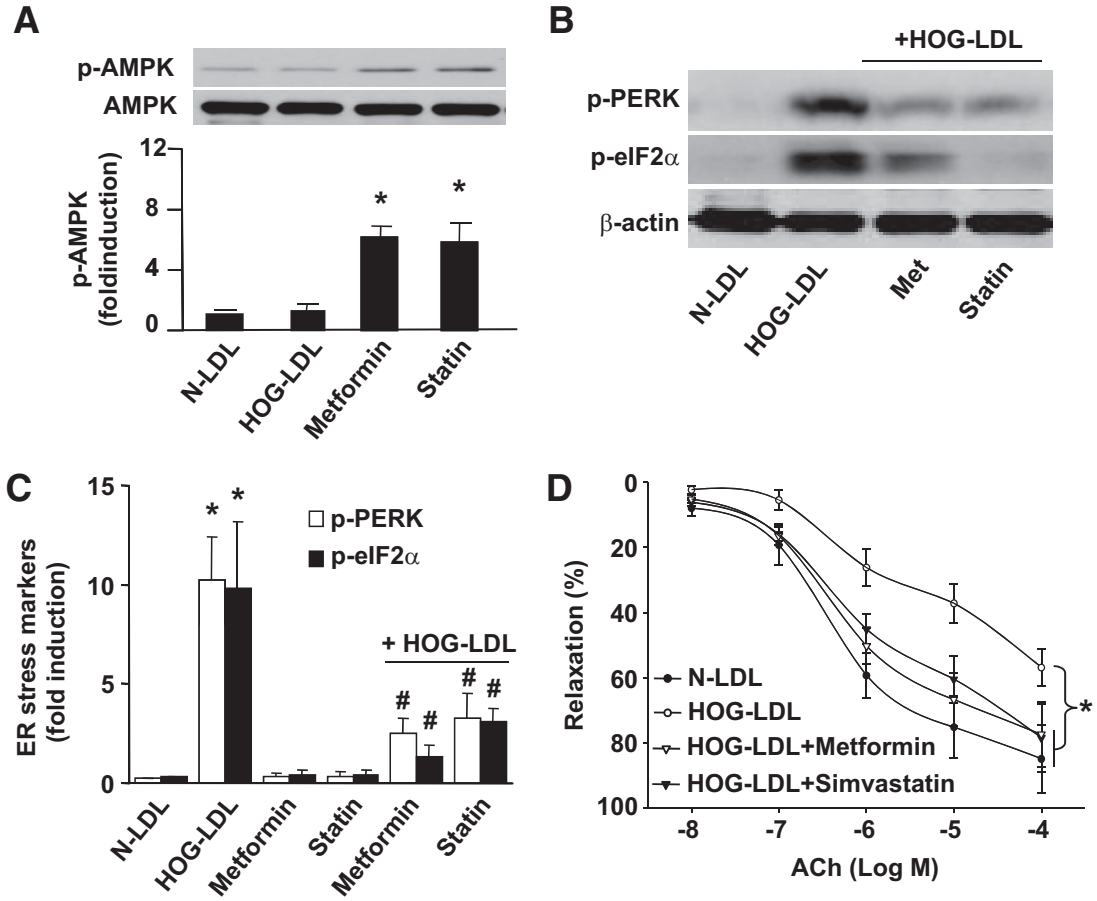

FIG. 6. Genetic activation or inhibition of AMPK alters HOG-LDL–induced ER stress in ex vivo aortae. *A*: Aortic rings were cut (~3-mm length) and pretreated with 2 mmol/l metformin or 50 μmol/l simvastatin for 30 min, followed by addition of 100 μg/ml HOG-LDL or N-LDL (latter as control), with or without metformin or statin for up to 6 h. *$P < 0.05$ metformin or statin vs. controls; #$P < 0.05$ controls vs. metformin plus HOG-LDL or statin plus HOG-LDL. *B* and *C*: ER stress markers were detected from set (*A*); $n \geq 4$ in each treatment. *$P < 0.01$ HOG-LDL vs. N-LDL; #$P < 0.01$ HOG-LDL+metformin or HOG-LDL+statin vs. HOG-LDL alone. *D*: HOG-LDL impaired aortic relaxation, which can be restored by metformin or statin. $n = 4$ in each group. *$P < 0.05$ HOG-LDL vs. N-LDL or HOG-LDL+metformin or HOG-LDL+statin.

creased cholesterol levels in ApoE$^{-/-}$/AMPKα2$^{-/-}$ mice (Table 1).

DISCUSSION

In this study, we have demonstrated that LDL oxidation and glycation cause aberrant ER stress via the oxidation of SERCA in endothelial cells. We have also provided evidence that AMPK activation is effective in inhibiting HOG-LDL–enhanced SERCA oxidation and consequent ER stress in vivo. Finally, we found chronic administration of Tempol restored SERCA activity, ER stress, endothelium function, and atherosclerosis caused by HFD in vivo.

One of the most important findings in the present study is that HOG-LDL increases ER stress by ROS-dependent oxidation and inhibition of SERCA activity, a key enzyme that controls intracellular [Ca^{2+}] (34,36–39). We have further found HOG-LDL increases the oxidation of Cys674, a known site for SERCA glutathiolation and oxidation, likely via NAD(P)H oxidase–derived ROSs. Our observations are in line with several published studies that have demonstrated that SERCA is prone to oxidation at one of its thiol groups under certain conditions (30,40,41) and that its oxidation is significantly increased in atherosclerotic lesions (41). Importantly, we found that chronic administration of Tempol significantly inhibited ER stress, endothelial dysfunction, and aortic lesions in vivo. Our results are also consistent with a recent report in which antioxidant metallothionein is reported to inhibit ER stress caused by diabetes and angiotensin II (42). Thus, ROS might be a common ER stress inducer in different cell types including endothelial cells, vascular smooth muscle cells, and myocytes.

Another important finding of the present study is that AMPK activation suppresses ER stress by inhibiting NAD(P)H oxidase–derived ROSs, a well-known ER stress initiator that has been implicated in the progression of atherosclerosis in many studies (43–46). Our unpublished data suggest that AMPKα2 deletion increases the expression of NAD(P)H oxidase subunits and NAD(P)H oxidase–derived ROSs in endothelial cells. How AMPK suppresses NAD(P)H oxidase remains undefined but warrants further investigation.

Circulating levels of oxidized LDL have been proposed to be a predictor of secondary cardiovascular events (47,48). Plasma levels of oxidized LDL correlate with endothelial dysfunction and are reduced after lipid-lowering therapy using apheresis or statins (49). The concentration of oxidized and oxidized glycated LDL in the circulation in healthy individuals is thought to be low (1–5 μg protein/ml). Because conventional lipid profiles are often abnormal in type 2 diabetes including increased triglycerides, normal or elevated levels of LDL, and re-

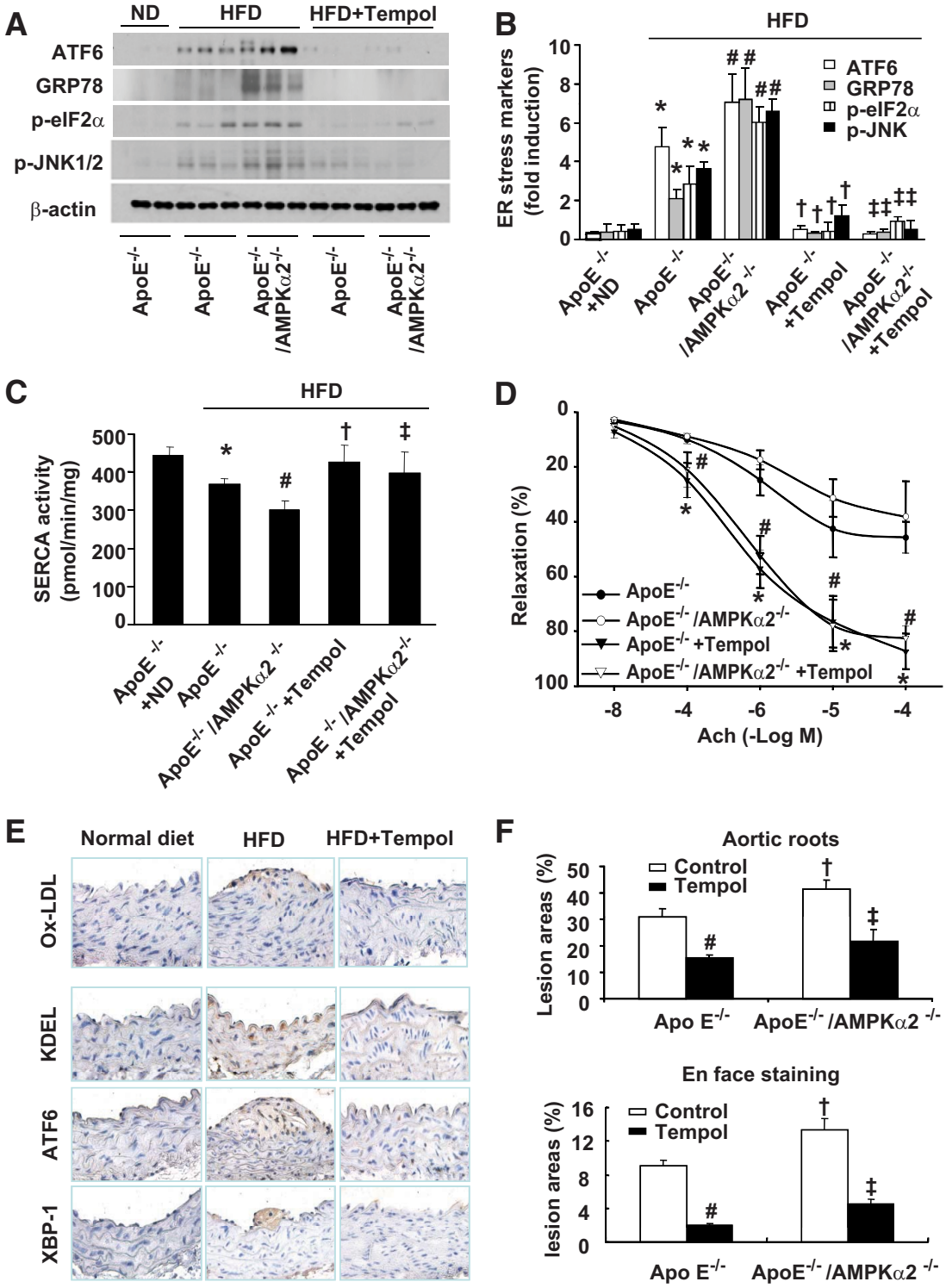

FIG. 7. Inhibition of SERCA oxidation by antioxidant Tempol reduced ER stress and atherosclerosis in vivo. *A* and *B*: Supplement of antioxidant Tempol significantly reduced ER stress. ApoE$^{-/-}$ and ApoE$^{-/-}$/AMPKα2$^{-/-}$ mice exhibited ER stress when fed with HFD compared with ApoE$^{-/-}$ mice fed with normal diet (ND) or HFD, as described in the "Research Design and Methods" section. $n = 5$. *$P < 0.05$ ApoE$^{-/-}$ with HFD vs. ApoE$^{-/-}$ with ND; #$P < 0.05$ ApoE$^{-/-}$/AMPKα2$^{-/-}$ with HFD vs. ApoE$^{-/-}$ with HFD; †$P < 0.05$ ApoE$^{-/-}$ with HFD vs. Tempol-treated ApoE$^{-/-}$ with HFD; ‡$P < 0.05$ ApoE$^{-/-}$/AMPKα2$^{-/-}$ plus HFD vs. Tempol-treated ApoE$^{-/-}$/AMPKα2$^{-/-}$ with HFD. *C*: Tempol supplementation protects aortic SERCA activity in vivo. $n = 5$. *$P < 0.05$ ApoE$^{-/-}$ with HFD vs. ApoE$^{-/-}$ with ND; #$P < 0.05$ ApoE$^{-/-}$/AMPKα2$^{-/-}$ with HFD vs. ApoE$^{-/-}$ with HFD; †$P < 0.05$ ApoE$^{-/-}$ with HFD vs. Tempol-treated ApoE$^{-/-}$ with HFD; ‡$P < 0.05$ ApoE$^{-/-}$/AMPKα2$^{-/-}$/HFD vs. Tempol-treated ApoE$^{-/-}$/AMPKα2$^{-/-}$ with HFD. *D*: Tempol supplement ablates HFD-induced reduction of acetylcholine-induced endothelium-dependent vasorelaxation in isolated mouse aortae from ApoE$^{-/-}$/AMPKα2$^{-/-}$ with HFD vs. ApoE$^{-/-}$ with HFD. *$P < 0.05$ ApoE$^{-/-}$ with HFD vs. Tempol-treated ApoE$^{-/-}$ with HFD; #$P < 0.05$ ApoE$^{-/-}$/AMPKα2$^{-/-}$ vs. Tempol-treated ApoE$^{-/-}$/AMPKα2$^{-/-}$ with HFD. *E*: Tempol administration reduces ox-LDL, ER stress, and aortic lesion progression in ApoE$^{-/-}$ mice detected by immunostaining; $n \geq 4$ in each group. *F*: Tempol administration inhibits aortic lesions in aortic roots and aortic arches (en face staining); $n \geq 5$ in each group. # and ‡ indicate $P < 0.05$ Tempol treatment vs. control in each group; †$P < 0.05$ ApoE$^{-/-}$/AMPKα2$^{-/-}$ vs. ApoE$^{-/-}$ in each group. (A high-quality digital representation of this figure is available in the online issue.)

TABLE 1
Plasma lipids and glucose in ApoE$^{-/-}$ and ApoE$^{-/-}$/AMPKα2$^{-/-}$ mice

	Without Tempol		With Tempol	
	ApoE$^{-/-}$	ApoE$^{-/-}$/AMPKα2$^{-/-}$	ApoE$^{-/-}$	ApoE$^{-/-}$/AMPKα2$^{-/-}$
Glucose (mg/dl)	155.8 ± 9.0	168.1 ± 16.8	125.0 ± 11.2	183.3 ± 13.7
Cholesterol (mmol/l)	17.6 ± 1.1	15.4 ± 1.2	20.2 ± 0.9	26.1 ± 0.9*
Triglyceride (mmol/l)	1.11 ± 0.17	1.07 ± 0.19	0.92 ± 0.09	1.31 ± 0.09

Values are mean ± SE. n = 5–10 per group; *$P < 0.05$ vs. ApoE$^{-/-}$. Mice underwent a 14- to 15-h fast before blood samples were collected. Blood glucose levels were determined by applying tail blood to an OneTouch Ultra Blood Glucose Monitoring System (LifeScan). Serum cholesterol and triglyceride levels were measured enzymatically, using Infinity reagents from Thermo DMA according to the manufacturer's instructions.

duced HDL, it is expected that glycation and oxidation of LDL are enhanced by diabetes. Further, the levels of HOG-LDL are likely to be much higher in the extravascular environment such as aortic lesions, when LDLs are retained in a less antioxidant-rich milieu and exposed to pro-oxidant stresses. For example, Nishi et al. demonstrated that in the general population, levels of oxidized LDL are ~70-fold higher in arterial lesions than in the circulation (50). For these reasons, we consider the concentrations of LDL proposed in this work to be a reasonable estimate of those present in vivo. Thus, our findings might be important for understanding the etiology of atherosclerosis.

In summary, the present study has demonstrated that activation of AMPK suppresses HOG-LDL–induced ER stress by inhibiting NAD(P)H oxidase–derived ROS and SERCA oxidation. Therefore, AMPK may be a physiological regulator that maintains ER homeostasis and endothelial function. The proposed mechanism is outlined in supplementary Fig. 4.

ACKNOWLEDGMENTS

This study was supported by National Institutes of Health (NIH) grants (HL079584, HL080499, and HL096032), the Juvenile Diabetes Research Foundation, and the American Diabetes Association to M.-H.Z., and by grants from the American Diabetes Association (1-05-RA-74) and the Oklahoma Center for the Advancement of Science and Technology (HR08-67; NIH P20RR024215) to T.J.L. M.-H.Z. is a recipient of the National Established Investigator Award from the American Heart Association.

No potential conflicts of interest relevant to this article were reported.

We thank Drs. Najeeb Shirwany for his assistance in article preparation and Leonidas Tsiokas for technical support in ratiometric analysis of intracellular calcium.

REFERENCES

1. Cominacini L, Pasini AF, Garbin U, Davoli A, Tosetti ML, Campagnola M, Rigoni A, Pastorino AM, Lo Cascio V, Sawamura T. Oxidized low density lipoprotein (ox-LDL) binding to ox-LDL receptor-1 in endothelial cells induces the activation of NF-kappaB through an increased production of intracellular reactive oxygen species. J Biol Chem 2000;275:12633–12638
2. Littlewood TD, Bennett MR. Apoptotic cell death in atherosclerosis. Curr Opin Lipidol 2003;14:469–475
3. Brownlee M. Advanced protein glycosylation in diabetes and aging. Annu Rev Med 1995;46:223–234
4. Kennedy AL, Lyons TJ. Glycation, oxidation, and lipoxidation in the development of diabetic complications. Metabolism 1997;46:14–21
5. Gugliucci Creriche A, Dumont S, Siffert JC, Stahl AJ. In vitro glycated low-density lipoprotein interaction with human monocyte-derived macrophages. Res Immunol 1992;143:17–23
6. Kobayashi K, Watanabe J, Umeda F, Nawata H. Glycation accelerates the oxidation of low density lipoprotein by copper ions. Endocr J 1995;42:461–465
7. Millican SA, Schultz D, Bagga M, Coussons PJ, Müller K, Hunt JV. Glucose-modified low density lipoprotein enhances human monocyte chemotaxis. Free Radic Res 1998;28:533–542
8. Imanaga Y, Sakata N, Takebayashi S, Matsunaga A, Sasaki J, Arakawa K, Nagai R, Horiuchi S, Itabe H, Takano T. In vivo and in vitro evidence for the glycoxidation of low density lipoprotein in human atherosclerotic plaques. Atherosclerosis 2000;150:343–355
9. Palinski W, Koschinsky T, Butler SW, Miller E, Vlassara H, Cerami A, Witztum JL. Immunological evidence for the presence of advanced glycosylation end products in atherosclerotic lesions of euglycemic rabbits. Arterioscler Thromb Vasc Biol 1995;15:571–582
10. Adams MR, Kinlay S, Blake GJ, Orford JL, Ganz P, Selwyn AP. Atherogenic lipids and endothelial dysfunction: mechanisms in the genesis of ischemic syndromes. Annu Rev Med 2000;51:149–167
11. Napoli C. Oxidation of LDL, atherogenesis, and apoptosis. Ann N Y Acad Sci 2003;1010:698–709
12. Artwohl M, Graier WF, Roden M, Bischof M, Freudenthaler A, Waldhäusl W, Baumgartner-Parzer SM. Diabetic LDL triggers apoptosis in vascular endothelial cells. Diabetes 2003;52:1240–1247
13. de Nigris F, Tajana G, Condorelli M, D'Armiento FP, Sica G, Lerman LO, Napoli C. Glycoxidation of low-density lipoprotein increases TUNEL positivity and CPP32 activation in human coronary cells. Ann N Y Acad Sci 2003;1010:710–715
14. Taguchi S, Oinuma T, Yamada T. A comparative study of cultured smooth muscle cell proliferation and injury, utilizing glycated low density lipoproteins with slight oxidation, auto-oxidation, or extensive oxidation. J Atheroscler Thromb 2000;7:132–137
15. Eizirik DL, Cardozo AK, Cnop M. The role for endoplasmic reticulum stress in diabetes mellitus. Endocr Rev 2008;29:42–61
16. Ozcan U, Cao Q, Yilmaz E, Lee AH, Iwakoshi NN, Ozdelen E, Tuncman G, Görgün C, Glimcher LH, Hotamisligil GS. Endoplasmic reticulum stress links obesity, insulin action, and type 2 diabetes. Science 2004;306:457–461
17. Hotamisligil GS. Inflammation and endoplasmic reticulum stress in obesity and diabetes. Int J Obes (Lond) 2008;7(Suppl.):S52–S54
18. Erbay E, Babaev VR, Mayers JR, Makowski L, Charles KN, Snitow ME, Fazio S, Wiest MM, Watkins SM, Linton MF, Hotamisligil GS. Reducing endoplasmic reticulum stress through a macrophage lipid chaperone alleviates atherosclerosis. Nat Med 2009;15:1383–1391
19. Xu C, Bailly-Maitre B, Reed JC. Endoplasmic reticulum stress: cell life and death decisions. J Clin Invest 2005;115:2656–2664
20. Ye Y, Shibata Y, Yun C, Ron D, Rapoport TA. A membrane protein complex mediates retro-translocation from the ER lumen into the cytosol. Nature 2004;429:841–847
21. Hardie DG. AMP-activated/SNF1 protein kinases: conserved guardians of cellular energy. Nat Rev Mol Cell Biol 2007;8:774–785
22. Hardie DG. Roles of the AMP-activated/SNF1 protein kinase family in the response to cellular stress. Biochem Soc Symp 1999;64:13–27
23. Kuramoto N, Wilkins ME, Fairfax BP, Revilla-Sanchez R, Terunuma M, Tamaki K, Iemata M, Warren N, Couve A, Calver A, Horvath Z, Freeman K, Carling D, Huang L, Gonzales C, Cooper E, Smart TG, Pangalos MN, Moss SJ. Phospho-dependent functional modulation of GABA(B) receptors by the metabolic sensor AMP-dependent protein kinase. Neuron 2007;53:233–247
24. Zou MH, Wu Y. AMP-activated protein kinase activation as a strategy for protecting vascular endothelial function. Clin Exp Pharmacol Physiol 2008;35:535–545
25. Davis BJ, Xie Z, Viollet B, Zou MH. Activation of the AMP-activated kinase by antidiabetes drug metformin stimulates nitric oxide synthesis in vivo by promoting the association of heat shock protein 90 and endothelial nitric oxide synthase. Diabetes 2006;55:496–505
26. Terai K, Hiramoto Y, Masaki M, Sugiyama S, Kuroda T, Hori M, Kawase I, Hirota H. AMP-activated protein kinase protects cardiomyocytes against

hypoxic injury through attenuation of endoplasmic reticulum stress. Mol Cell Biol 2005;25:9554–9575
27. Dong Y, Wu Y, Wu M, Wang S, Zhang J, Xie Z, Xu J, Song P, Wilson K, Zhao Z, Lyons T, Zou MH. Activation of protease calpain by oxidized and glycated LDL increases the degradation of endothelial nitric oxide synthase. J Cell Mol Med 2009;13:2899–2910
28. Klein RL, Semler AJ, Baynes JW, Thorpe SR, Lyons TJ, Jenkins AJ. Glycation does not alter LDL-induced secretion of tissue plasminogen activator and plasminogen activator inhibitor-1 from human aortic endothelial cells. Ann N Y Acad Sci 2005;1043:379–389
29. Authi KS, Bokkala S, Patel Y, Kakkar VV, Munkonge F. Ca2+ release from platelet intracellular stores by thapsigargin and 2,5-di-(t-butyl)-1,4-benzohydroquinone: relationship to Ca2+ pools and relevance in platelet activation. Biochem J 1993;294(Pt. 1):119–126
30. Tong X, Ying J, Pimentel DR, Trucillo M, Adachi T, Cohen RA. High glucose oxidizes SERCA cysteine-674 and prevents inhibition by nitric oxide of smooth muscle cell migration. J Mol Cell Cardiol 2008;44:361–369
31. Ma R, Li WP, Rundle D, Kong J, Akbarali HI, Tsiokas L. PKD2 functions as an epidermal growth factor-activated plasma membrane channel. Mol Cell Biol 2005;25:8285–8298
32. Fernández-Hernando C, Ackah E, Yu J, Suárez Y, Murata T, Iwakiri Y, Prendergast J, Miao RQ, Birnbaum MJ, Sessa WC. Loss of Akt1 leads to severe atherosclerosis and occlusive coronary artery disease. Cell Metab 2007;6:446–457
33. Cnop M, Welsh N, Jonas JC, Jorns A, Lenzen S, Eizirik DL. Mechanisms of pancreatic beta-cell death in type 1 and type 2 diabetes: many differences, few similarities. Diabetes 2005;2(Suppl.):S97–S107
34. Cardozo AK, Ortis F, Storling J, Feng YM, Rasschaert J, Tonnesen M, Van Eylen F, Mandrup-Poulsen T, Herchuelz A, Eizirik DL. Cytokines downregulate the sarcoendoplasmic reticulum pump Ca2+ ATPase 2b and deplete endoplasmic reticulum Ca2+, leading to induction of endoplasmic reticulum stress in pancreatic beta-cells. Diabetes 2005;54:452–461
35. Xie Z, Zhang J, Wu J, Viollet B, Zou MH. Upregulation of mitochondrial uncoupling protein-2 by the AMP-activated protein kinase in endothelial cells attenuates oxidative stress in diabetes. Diabetes 2008;57:3222–3230
36. Caspersen C, Pedersen PS, Treiman M. The sarco/endoplasmic reticulum calcium-ATPase 2b is an endoplasmic reticulum stress-inducible protein. J Biol Chem 2000;275:22363–22372
37. Denmeade SR, Isaacs JT. The SERCA pump as a therapeutic target: making a “smart bomb” for prostate cancer. Cancer Biol Ther 2005;4:14–22
38. Hojmann Larsen A, Frandsen A, Treiman M. Upregulation of the SERCA-type Ca2+ pump activity in response to endoplasmic reticulum stress in PC12 cells. BMC Biochem 2001;2:4
39. Takadera T, Fujibayashi M, Kaniyu H, Sakota N, Ohyashiki T. Caspase-dependent apoptosis induced by thapsigargin was prevented by glycogen synthase kinase-3 inhibitors in cultured rat cortical neurons. Neurochem Res 2007;32:1336–1342
40. Ying J, Sharov V, Xu S, Jiang B, Gerrity R, Schöneich C, Cohen RA. Cysteine-674 oxidation and degradation of sarcoplasmic reticulum Ca(2+) ATPase in diabetic pig aorta. Free Radic Biol Med 2008;45:756–762
41. Adachi T, Weisbrod RM, Pimentel DR, Ying J, Sharov VS, Schöneich C, Cohen RA. S-Glutathiolation by peroxynitrite activates SERCA during arterial relaxation by nitric oxide. Nat Med 2004;10:1200–1207
42. Xu J, Wang G, Wang Y, Liu Q, Xu W, Tan Y, Cai L. Diabetes- and angiotensin II-induced cardiac endoplasmic reticulum stress and cell death: metallothionein protection. J Cell Mol Med 2009;13:1499–1512
43. Barry-Lane PA, Patterson C, van der Merwe M, Hu Z, Holland SM, Yeh ET, Runge MS. p47phox is required for atherosclerotic lesion progression in ApoE(-/-) mice. J Clin Invest 2001;108:1513–1522
44. Cathcart MK. Regulation of superoxide anion production by NADPH oxidase in monocytes/macrophages: contributions to atherosclerosis. Arterioscler Thromb Vasc Biol 2004;24:23–28
45. Rueckschloss U, Duerrschmidt N, Morawietz H. NADPH oxidase in endothelial cells: impact on atherosclerosis. Antioxid Redox Signal 2003;5:171–180
46. Griendling KK, Harrison DG. Out, damned dot: studies of the NADPH oxidase in atherosclerosis. J Clin Invest 2001;108:1423–1424
47. Matsumoto T, Takashima H, Ohira N, Tarutani Y, Yasuda Y, Yamane T, Matsuo S, Horie M. Plasma level of oxidized low-density lipoprotein is an independent determinant of coronary macrovasomotor and microvasomotor responses induced by bradykinin. J Am Coll Cardiol 2004;44:451–457
48. Fraley AE, Tsimikas S. Clinical applications of circulating oxidized low-density lipoprotein biomarkers in cardiovascular disease. Curr Opin Lipidol 2006;17:502–509
49. Navab M, Ananthramaiah GM, Reddy ST, Van Lenten BJ, Ansell BJ, Fonarow GC, Vahabzadeh K, Hama S, Hough G, Kamranpour N, Berliner JA, Lusis AJ, Fogelman AM. The oxidation hypothesis of atherogenesis: the role of oxidized phospholipids and HDL. J Lipid Res 2004;45:993–1007
50. Nishi K, Itabe H, Uno M, Kitazato KT, Horiguchi H, Shinno K, Nagahiro S. Oxidized LDL in carotid plaques and plasma associates with plaque instability. Arterioscler Thromb Vasc Biol 2002;22:1649–1654